Topologies of Magnetic Flux-rope embedded in Coronal Mass Ejections

Teresa Nieves-Ch.
Neel P. Savani

Historical Context

Previously…

- Morrison, P., 1954. (Phys. Rev) **Solar-connected variation of the cosmic rays.**
- Montgomery et al. 1974 (JGR), **Positive evidence for closed magnetic structures in the solar wind associated with interplanetary shocks waves.**

JOURNAL OF GEOPHYSICAL RESEARCH, VOL. 86, NO. A8, PAGES 6673–6684, AUGUST 1, 1981

Magnetic Loop Behind an Interplanetary Shock: Voyager, Helios, and IMP 8 Observations

L. BURLAGA AND E. SITTLER

NASA Goddard Space Flight Center, Laboratory for Extraterrestrial Physics, Greenbelt, Maryland 20771

F. MARIANI

Istituto di Fisica Universita, Piazzale delle Scienze, Rome, Italy

R. SCHWENN

Max-Planck-Institut für Aeronomie, 3411 Katlenburg-Lindau 3, Federal Republic of Germany

Magnetic field and plasma data from five spacecraft (Voyager 1 and 2, Helios 1 and 2, and IMP 8) were used to analyze the flow behind an interplanetary shock. The shock was followed by a turbulent sheath in which there were large fluctuations in both the strength and the direction of the magnetic field. This in turn was followed by a region (magnetic cloud) in which the magnetic field vectors were observed to change by rotating nearly parallel to a plane, consistent with the passage of a magnetic loop. This loop extended at least 30° in longitude between 1 and 2 AU, and its radial dimension was approximately 0.5

MAGNETIC CLOUD DEFINITION

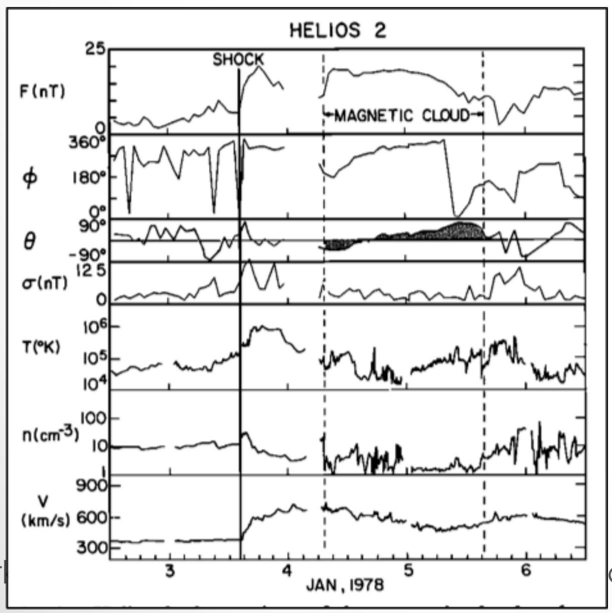

3D CONFIGURATION PROPOSED

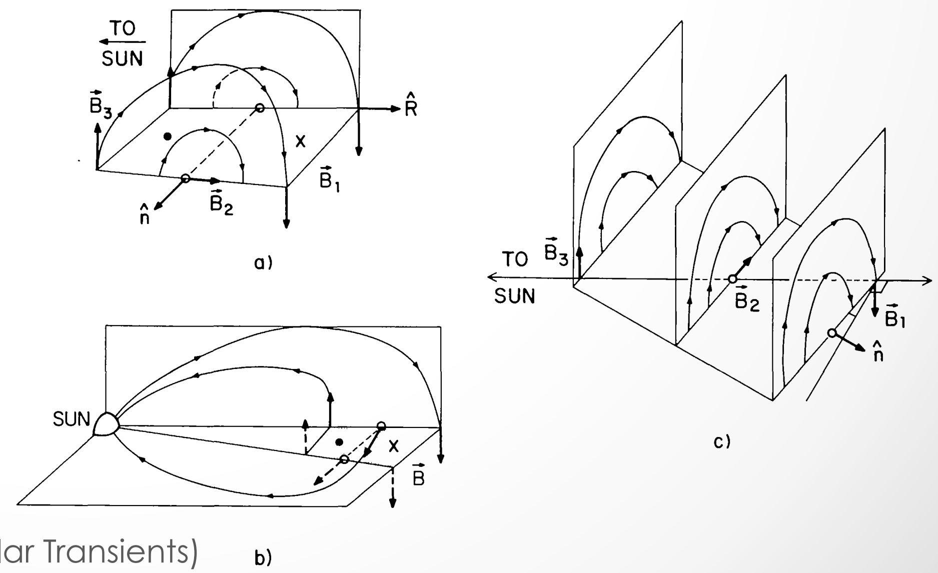

80’s, 90’s - *Top 10* magnetic topologies

1. **Goldstein 1983**
   (force-free concept)
2. **Marubashi 1986**
   (1st reconstruction)
3. **Burlaga 1988**
   (Lunquist 1950)
4. **Lepping et al. 1990**
   (reconstruction based on MVA)
5. **Vandas et al. 1991,1993**
   (reconstruction based on MVA
6. **Farrugia et al. 1992, 93, 95**
   (including expansion effect)
7. **Marubashi 1997**
   (Torus – curvature)
8. **Osherovich et al. 1999**
   (Multi-tube)
9. **Hidalgo et al. 2000**
   (non-force-free assumptions)
10. **Hu & Sonnerup, 2001**
   (Grad-Shafranov eq.)

THE MODEL

We assume that to a good approximation the magne
cloud is (magnetic) force-free, i.e., $J = \alpha B$, so that

$$\nabla \times B = J = \alpha B$$

This model, with variable α, was proposed by *Goldste*
[1983] and used by *Marubashi* [1986] to fit two magne
clouds. *Burlaga* [1988] showed that one can consider
approximately constant in describing magnetic clouds to fi
order. For constant α, equation (1) gives

$$\nabla \times (\nabla \times B) = \alpha(\nabla \times B) = \alpha^2 B$$

Models of magnetized plasma clouds 1149

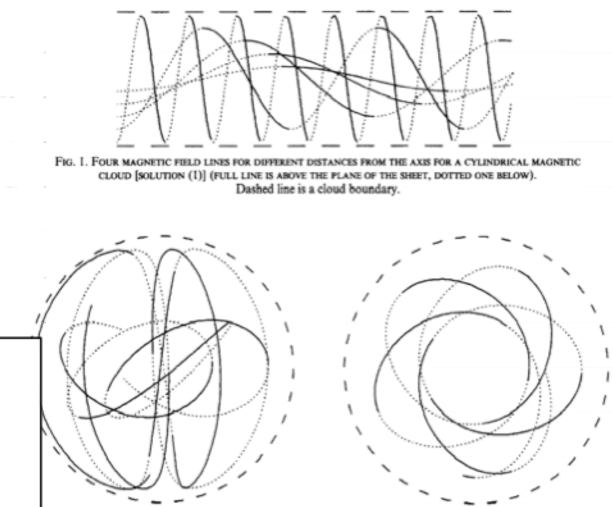

FIG. 1. FOUR MAGNETIC FIELD LINES FOR DIFFERENT DISTANCES FROM THE AXIS FOR A CYLINDRICAL MAGNETIC CLOUD [SOLUTION (1)] (FULL LINE IS ABOVE THE PLANE OF THE SHEET, DOTTED ONE BELOW). Dashed line is a cloud boundary.

2. TWO MAGNETIC FIELD LINES FOR THE DIFFERENT ING POINT LATITUDE FOR A SPHERICAL MAGNETIC CLOUD DAL SOLUTION (2)] (FULL LINE IS ABOVE THE PLANE OF THE SHEET, DOTTED ONE BELOW). Dashed line is a cloud boundary.

FIG. 3. A MAGNETIC FIELD LINE FOR A SPHERICAL MAGNETIC CLOUD [TOROIDAL SOLUTION (3)] (FULL LINE IS ABOVE THE PLANE OF THE SHEET, DOTTED ONE BELOW). Dashed line is a cloud boundary.

MAGNETIC CLOUD
(BURLAGA MODEL)

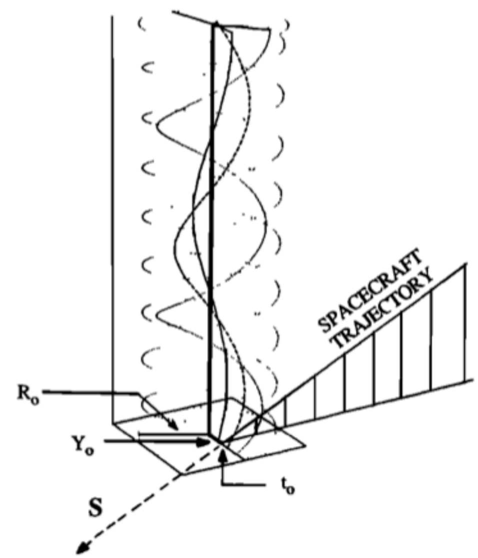

Ψ/Ψ_0

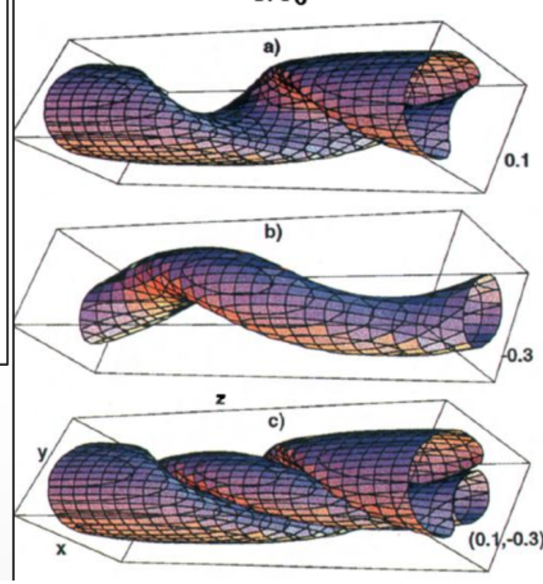

Why is it important to us?

JRNAL OF GEOPHYSICAL RESEARCH, VOL. 98, NO. A11, PAGES 18,937–18,949, NOVEMBER 1, 199

The Solar Flare Myth

J. T. GOSLING

Los Alamos National Laboratory, Los Alamos, New Mexico

Many years of research have demonstrated that large, nonrecurrent geomagnetic storms, shock wave disturbances in the solar wind, and energetic particle events in interplanetary space often occur in close association with large solar flares. This result has led to a paradigm of cause and effect - that large solar flares are the fundamental cause of these events in the near-Earth space environment. This paradigm, which I call "the solar flare myth," dominates the popular perception of the relationship between solar activity and interplanetary and geomagnetic events and has provided much of the pragmatic rationale for the study of the solar flare phenomenon. Yet there is good evidence that this paradigm is wrong and that flares do not generally play a central role in producing major transient disturbances in the near-Earth space environment. In this paper I outline a different paradigm of cause and effect that removes solar flares from their central position in the chain of events leading from the Sun to near-Earth space. Instead, this central role is given to events known as coronal mass ejections.

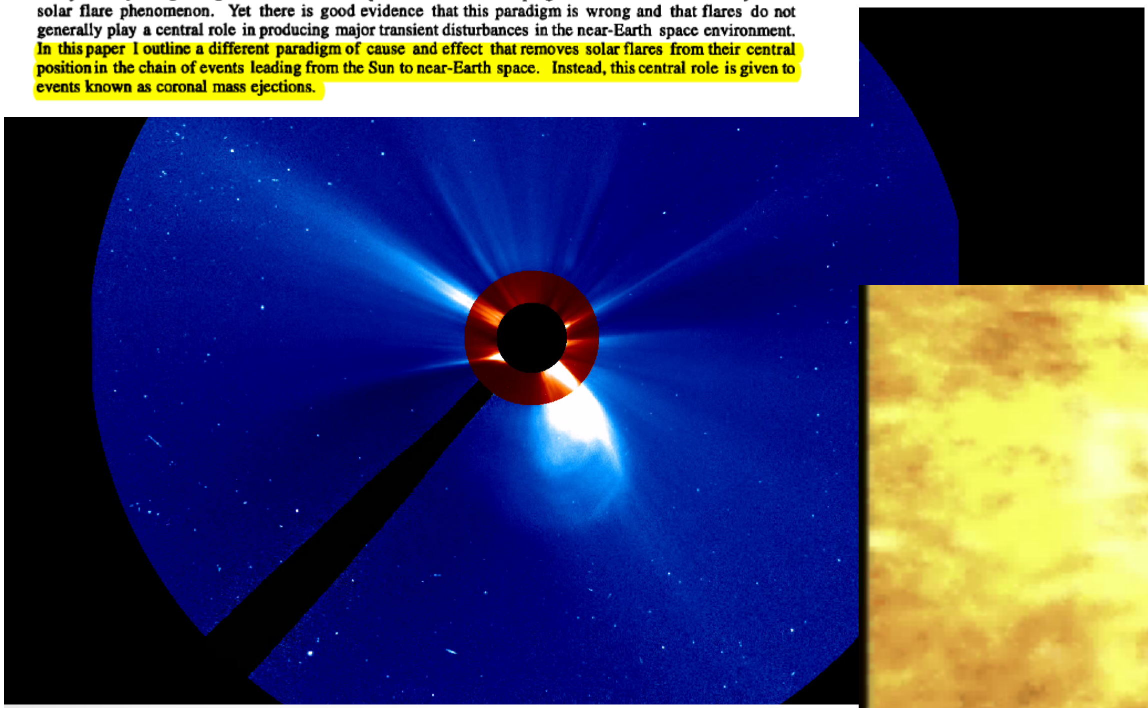

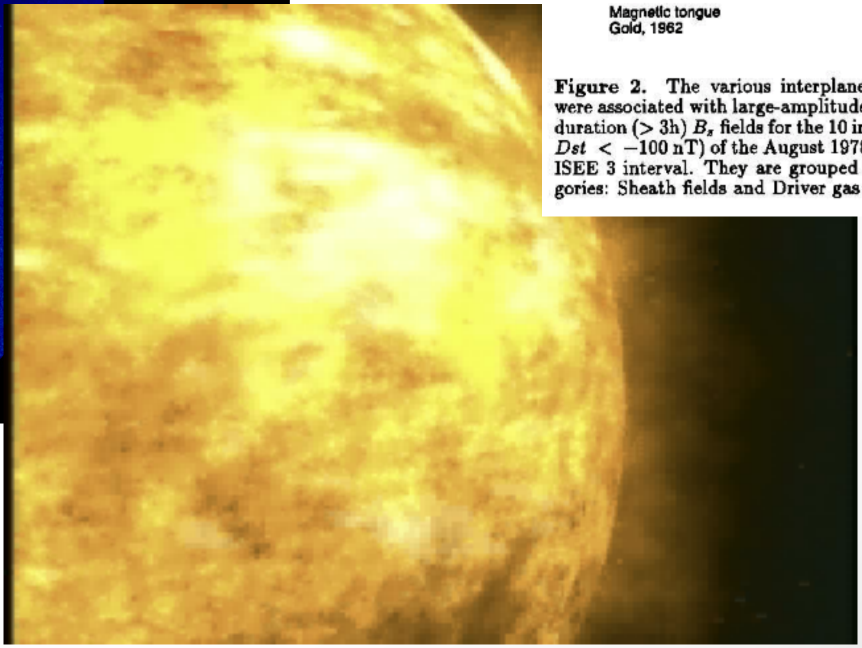

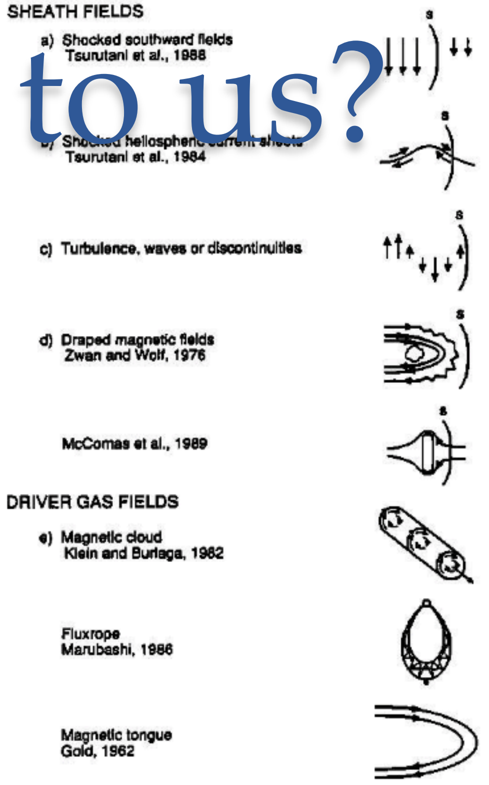

Figure 2. The various interplanetary features that were associated with large-amplitude (< −10 nT), long-duration (> 3h) B_s fields for the 10 intense storms (peak Dst < −100 nT) of the August 1978 to December 1979 ISEE 3 interval. They are grouped in two broad categories: Sheath fields and Driver gas fields.

Multi-view/point CME perspectives

INITIATION

BREAK OUT Models reproducing the three CME parts .. (Antiochos, 1998)

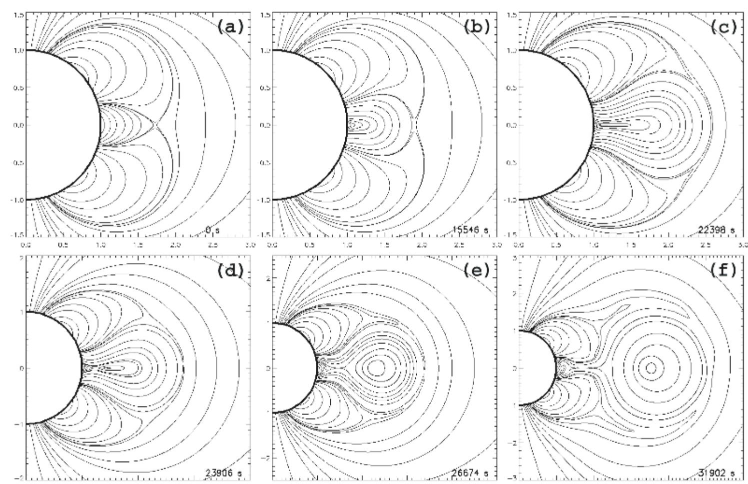

Lynch et al. 2014

MAGNETIC FLUX EMERGENCE from the solar convection zone could be the driver.. (Leake et al. 2014)

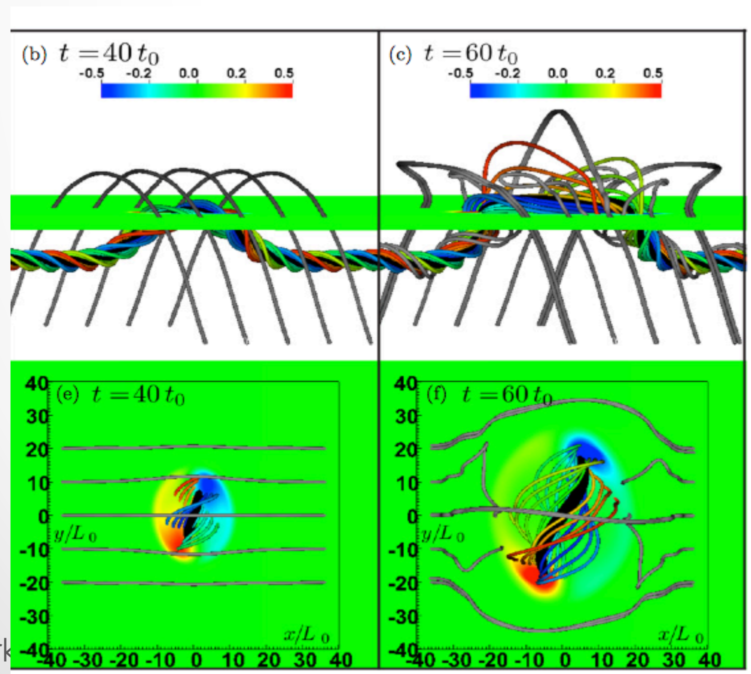

Multi-view/point CME perspectives

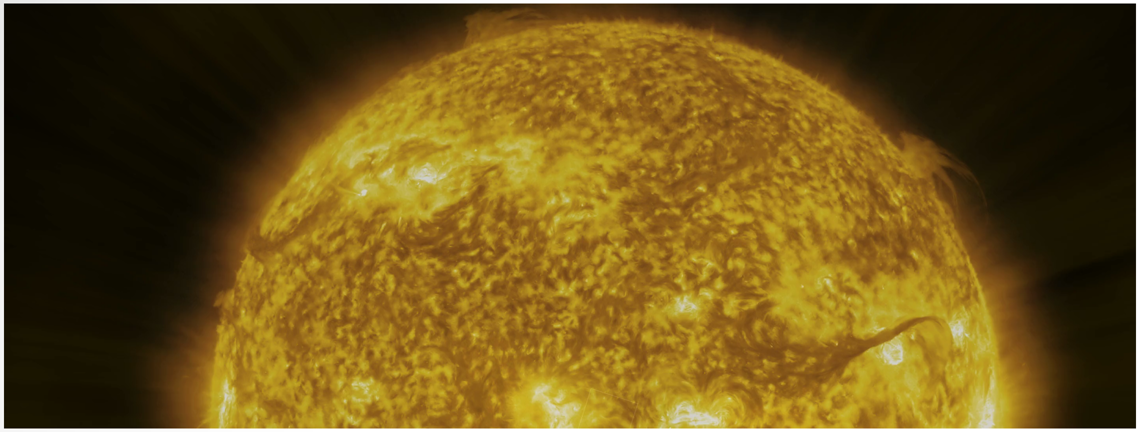

ERUPTION

PRE-FORMED CORONAL FLUX ROPE, e.g., Titov & Demoulin, 1999; Roussev et al. 2003; Török & Kliem 2005; Manchester et al. 2008

Titov & Demoulin, 1999

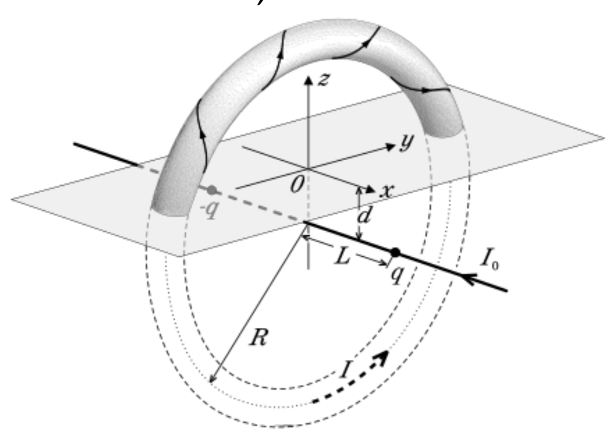

Fig. 2. The magnetic field under study is modeled by a force-free circular flux tube with the total current I, a pair of magnetic charges $-q$, q and a line current I_0. Below the photospheric plane $z = 0$ this configuration has no real physical meaning: it is used only to construct the proper magnetic field in corona.

Roussev et al. 2003

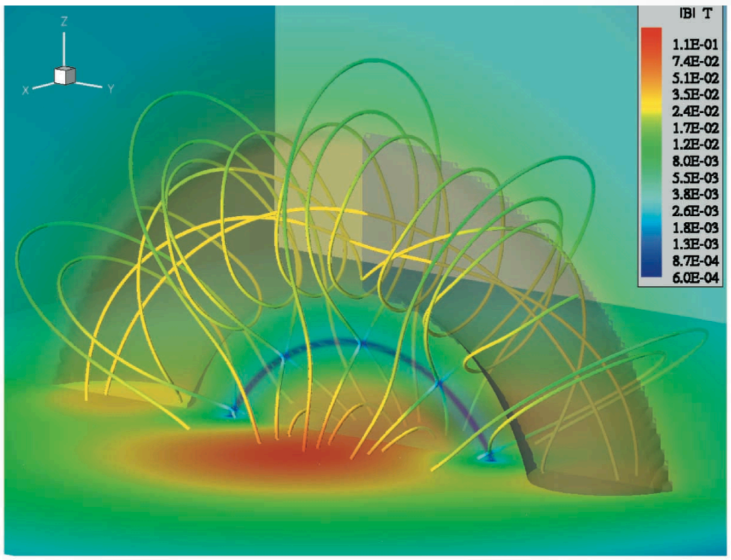

FIG. 1.—Three-dimensional view of the magnetic field configuration for the initial state. The solid lines are magnetic field lines, where the false-color code visualizes the magnetic field strength in units of tesla. The surface shaded in gray is an isosurface of $B_z = 0$.

Multi-view/point CME perspectives

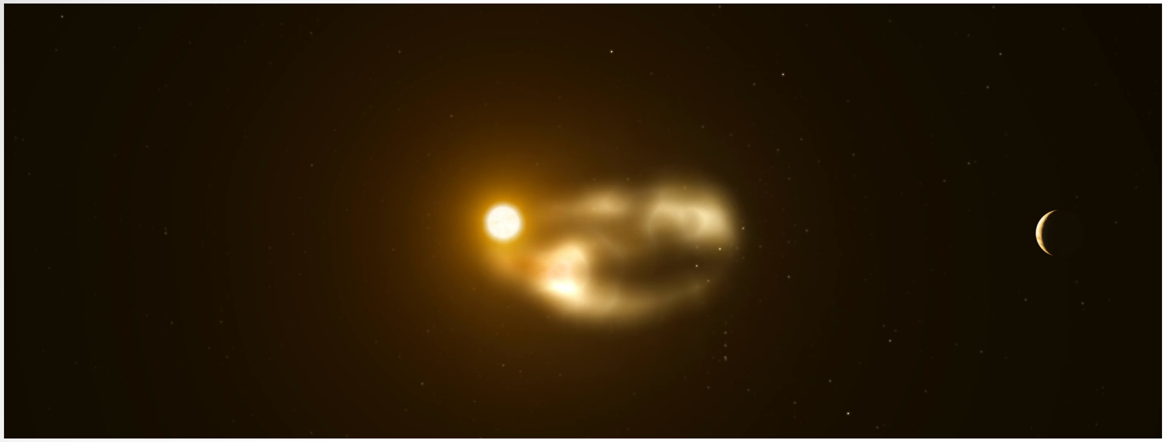

EVOLUTION out of the corona

PRE-FORMED CORONAL FLUX ROPE

Lugaz et al. 2005

Gibson & Low, 1998

3. THE THREE-DIMENSIONAL CME MODEL

The CME as an MHD phenomenon may be described by the following equations:

$$\rho\left[\frac{\partial \boldsymbol{v}}{\partial t} + (\boldsymbol{v}\cdot\nabla)\boldsymbol{v}\right] = \frac{1}{4\pi}(\nabla\times\boldsymbol{B})\times\boldsymbol{B} - \nabla p - \rho$$

$$\frac{\partial \rho}{\partial t} + \nabla\cdot(\rho\boldsymbol{v}) = 0\,,$$

$$\frac{\partial \boldsymbol{B}}{\partial t} = \nabla\times(\boldsymbol{v}\times\boldsymbol{B})\,,$$

$$\frac{\partial}{\partial t}(p\rho^{-\gamma}) + (\boldsymbol{v}\cdot\nabla)(p\rho^{-\gamma}) = 0\,,$$

3.1. *Self-similar Magnetohydrodynamics*

It is shown in Low (1984) that equations (1)–(4) admit time-dependent solutions with the radially directed flow

$$\boldsymbol{v} = r\,\frac{1}{\Phi_{ss}}\frac{d\Phi_{ss}}{dt}\,\hat{r}\,, \quad (5)$$

where Φ_{ss} is a function of time described by

$$\left(\frac{d\Phi_{ss}}{dt}\right)^2 = \frac{\eta\Phi_{ss} - 2\alpha}{\Phi_{ss}}\,, \quad (6)$$

η and α being constants. In this flow, the physical quantities evolve in a self-similar manner according to

$$\boldsymbol{B} = \frac{1}{\Phi_{ss}^2}\,H(\zeta, \theta, \phi)\,, \quad (7)$$

$$p = \frac{1}{\Phi_{ss}^4}\,P(\zeta, \theta, \phi)\,, \quad (8)$$

$$\rho = \frac{1}{\Phi_{ss}^3}\,D(\zeta, \theta, \phi)\,, \quad (9)$$

where the radial dependence is combined with time via the similarity variable

$$\zeta = \frac{r}{\Phi_{ss}}\,. \quad (10)$$

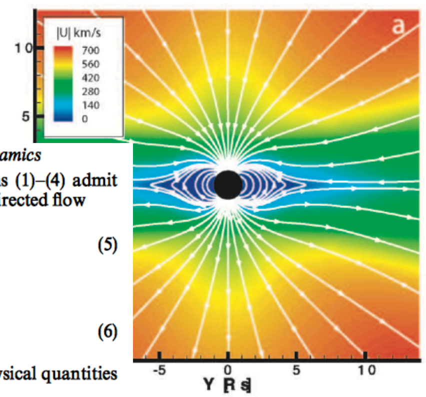

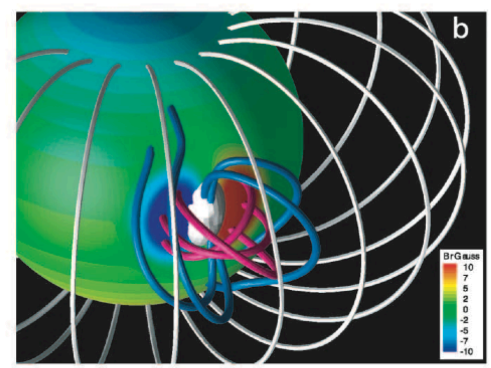

f the velocity magnitude of the steady state solar wind solution in the meridional (y-z) plane. "Streamlines" drawn in white illustrate eld in the plane. Note the bimodal nature of the solar wind speed. (*b*) Three-dimensional representation of the coronal magnetic field at ines. The flux rope is drawn with magenta and blue lines showing the toroidal and poloidal fields, respectively. The white surface is a ng to 2×10^{16} g cm^{-3} and showing the dense core contained in the GL flux rope. The false color sphere shows the magnetic field Sun for our model.

Multi-view/point CME perspectives

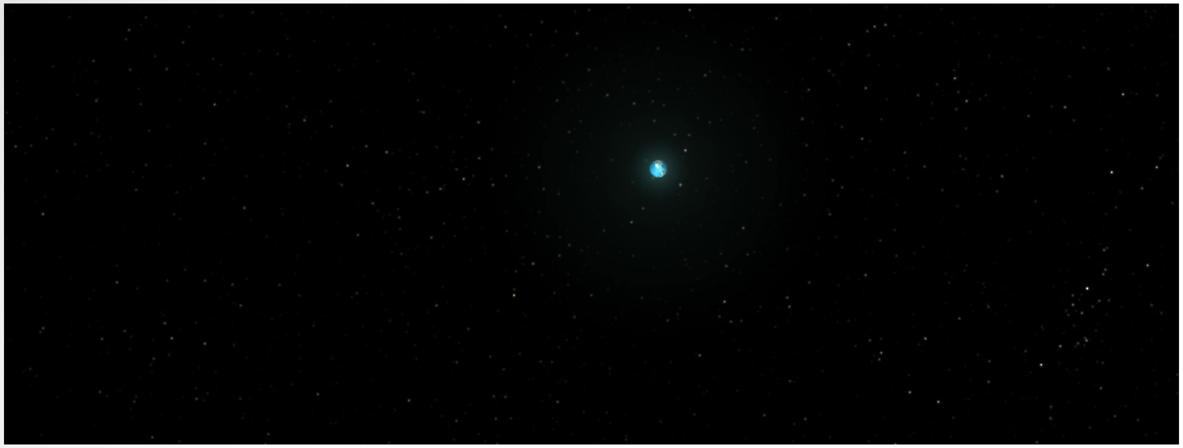

EVOLUTION in the inner heliosphere

Forward Modeling of CMEs using heliospheric imagers, Thernisien et al., 2006, 2011

Wood et al. 2009, 2011

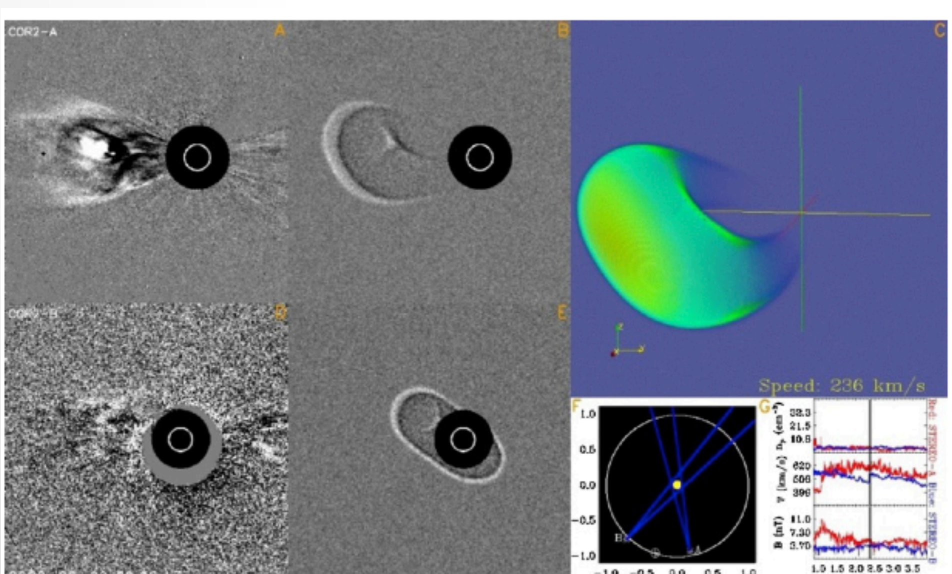

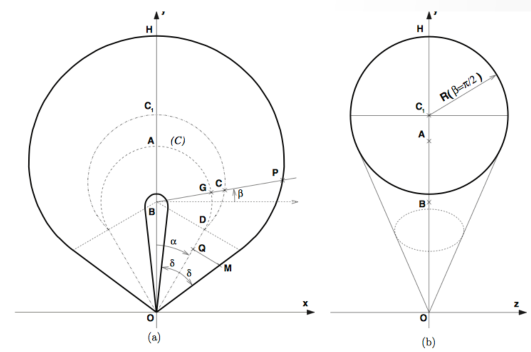

Figure 1. Schematic of the GCS model. The left panel shows a (O, x, y) planar cut of the croissant viewed face-on. The z-axis points toward the reader. The right panel shows a cut in the (O, y, z) plane where the croissant is viewed edge-on. In this view, only the circle (solid line) is in the (O, y, z) plane.

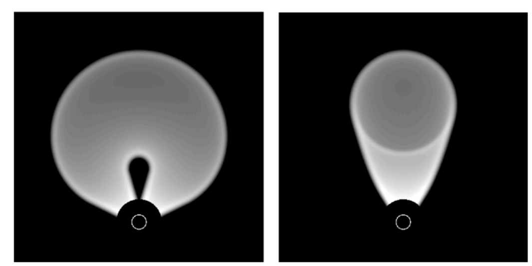

Figure 2. Rendered white-light images of the GCS model obtained by line-of-sight integration and using Thomson scattering (Billings 1966). The model orientations are the same as in Figure 1. Left: GCS model seen face-on. Right: GCS model seen edge-on.

Linking views

- Linking the remote and in-situ observations – big improvement in the time arrival and

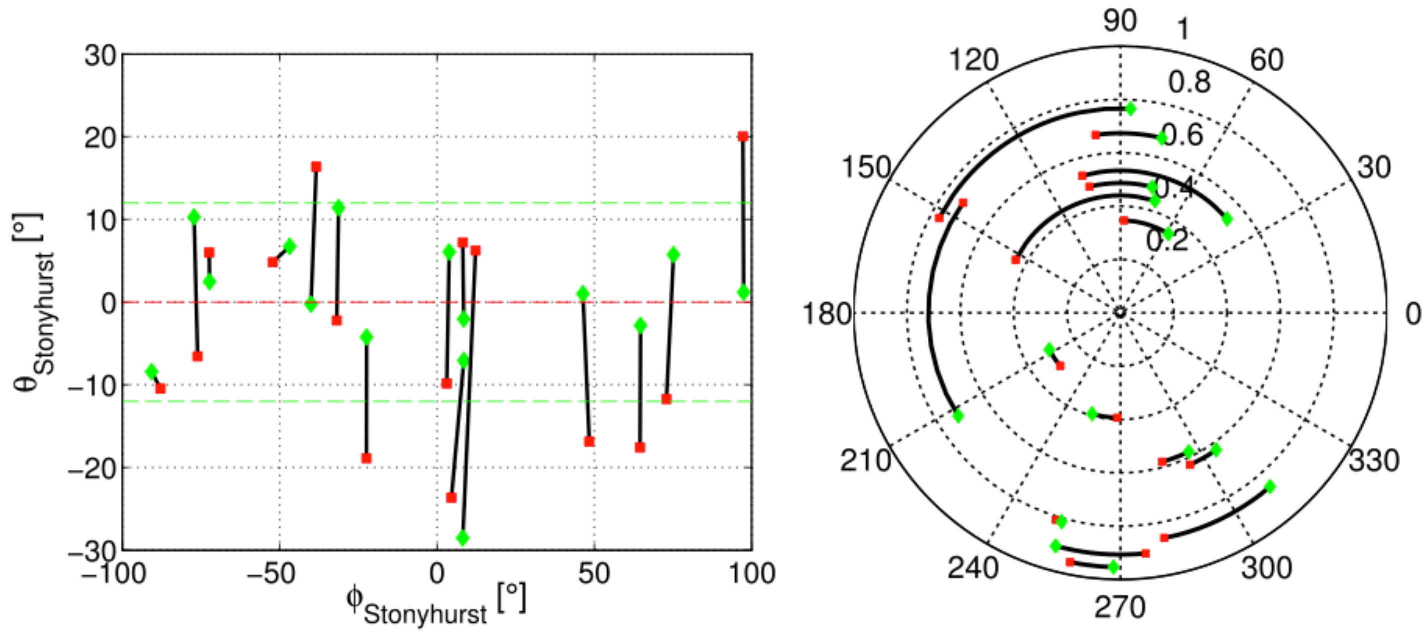

Figure 6 Diagrams of deflection (left) and rotation (right) of the studied MCs. Red squares denote the direction of MC propagation (left) and the direction of the normal to the MC plane (right) close to the Sun, *i.e.* in the initial position. Green diamonds denote the direction of MC propagation (left) and the direction of the normal to the MC plane (right) at 1 AU, *i.e.* in the final position.

Linking views – case by case

Farrugia et al. 2011

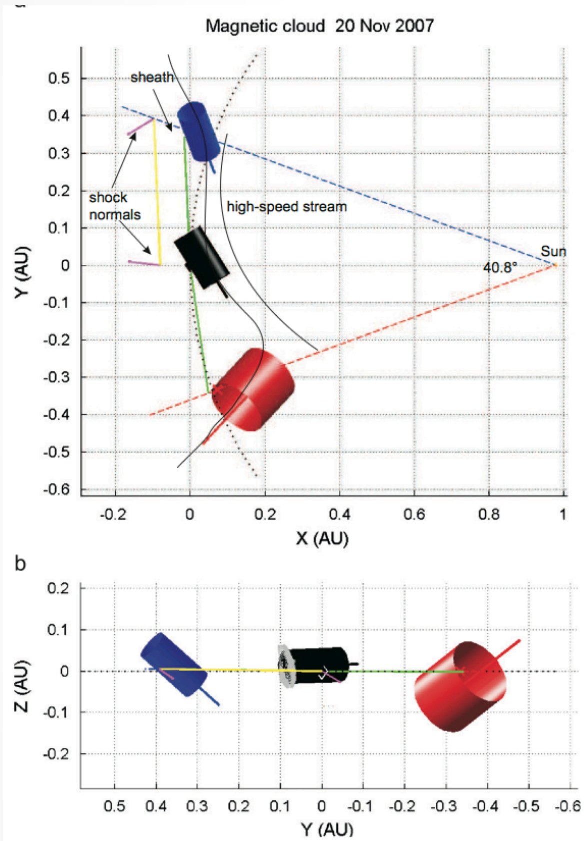

Nieves-Chinchilla. et al. 2012

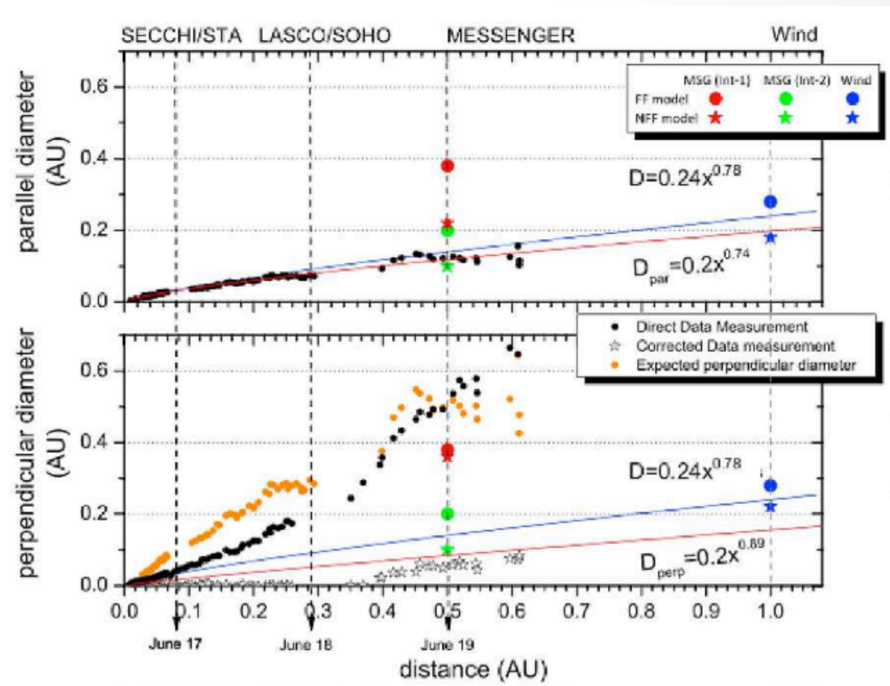

Linking views – case by case

Al-haddad. 2015, PhD.

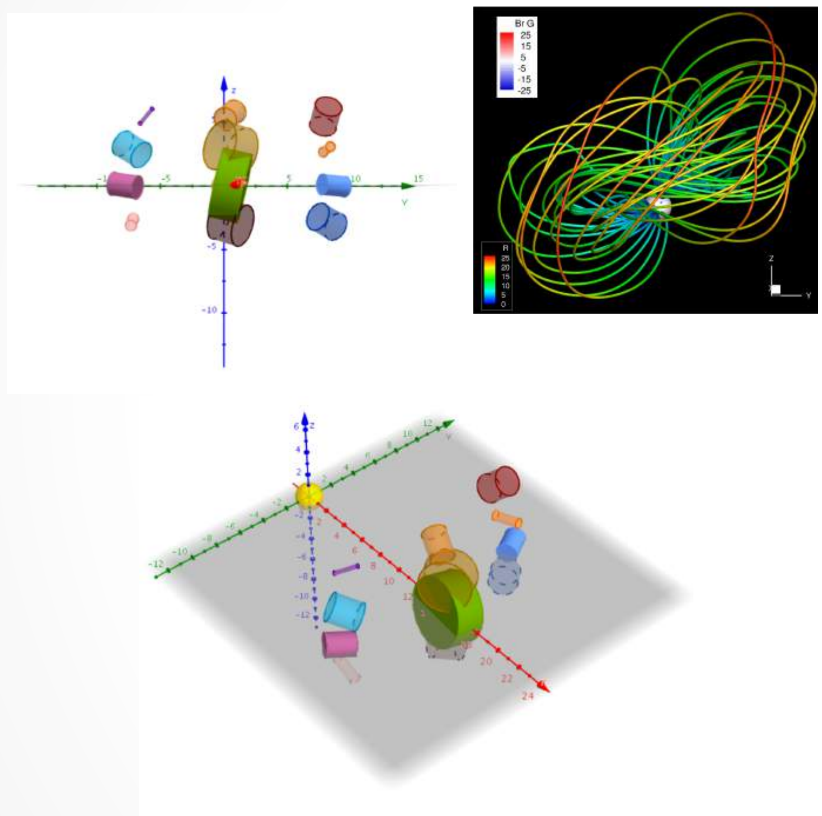

Figure 5.5: A global view of the the reconstructed cases for the writhe simulation. The top left panel provides a front view, from the direction of the propagation of the CME, of the reconstructed orientations and sizes. The top right panel shows the 3-D magnetic field lines from the simulation. The bottom panel provides a top view of the reconstructed cases.

QUESTION 1: Do we miss important information in the models assemble?

QUESTION 2: Do we need to revisit the models or the techniques?

QUESTION 3: New missions will be enough to reach the truly understanding of the ICMEs and the consequences of the journey throughout the heliosphere?

Are all the ICMEs magnetic flux-ropes structures?

Why some ICMEs are observed to MCs and others are not. Possible explanations:

1. An observational selection effect;
   - Observing limitation
2. Interactions of an erupting flux rope (FR) with itself or between neighboring FRs.
   - MC -> 0.77AU versus NoMC->0.73
3. Evolutionary process.
   - Analyzing *Helios* data, did not find a systematic trend in MC fraction and heliocentric distance.
4. >Two intrinsic initiation mechanisms
5. MCs are just an easily identifiable limit in an otherwise continuous spectrum of structures.
   - There are not proofs in the analysis to distinguish

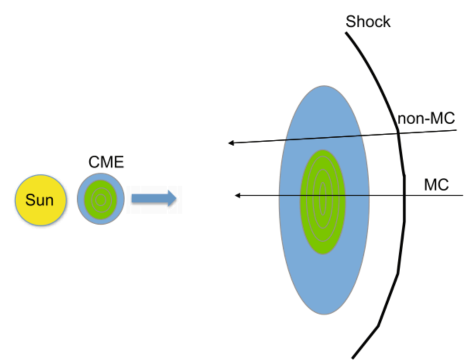

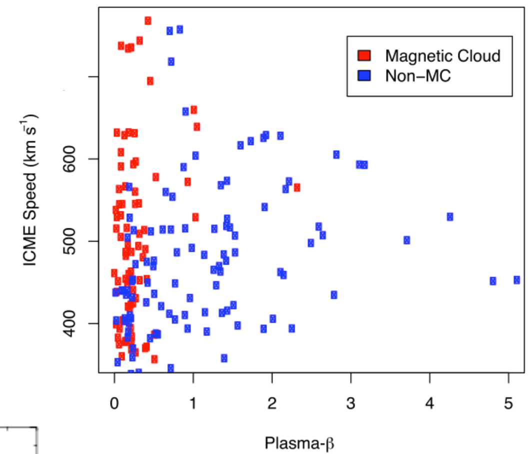

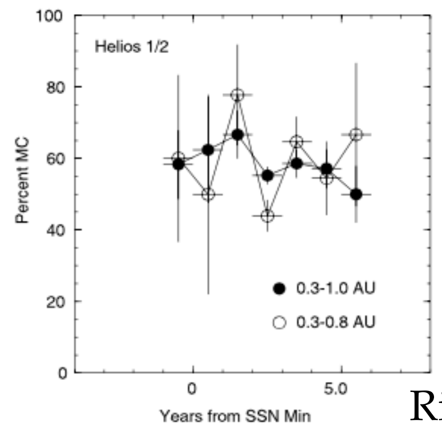

Richardson & Cane, 2004b

Two Coordinated Data Analysis Workshops (CDAWS), 2010-2011

ICME magnetic field configurations

Figure 1

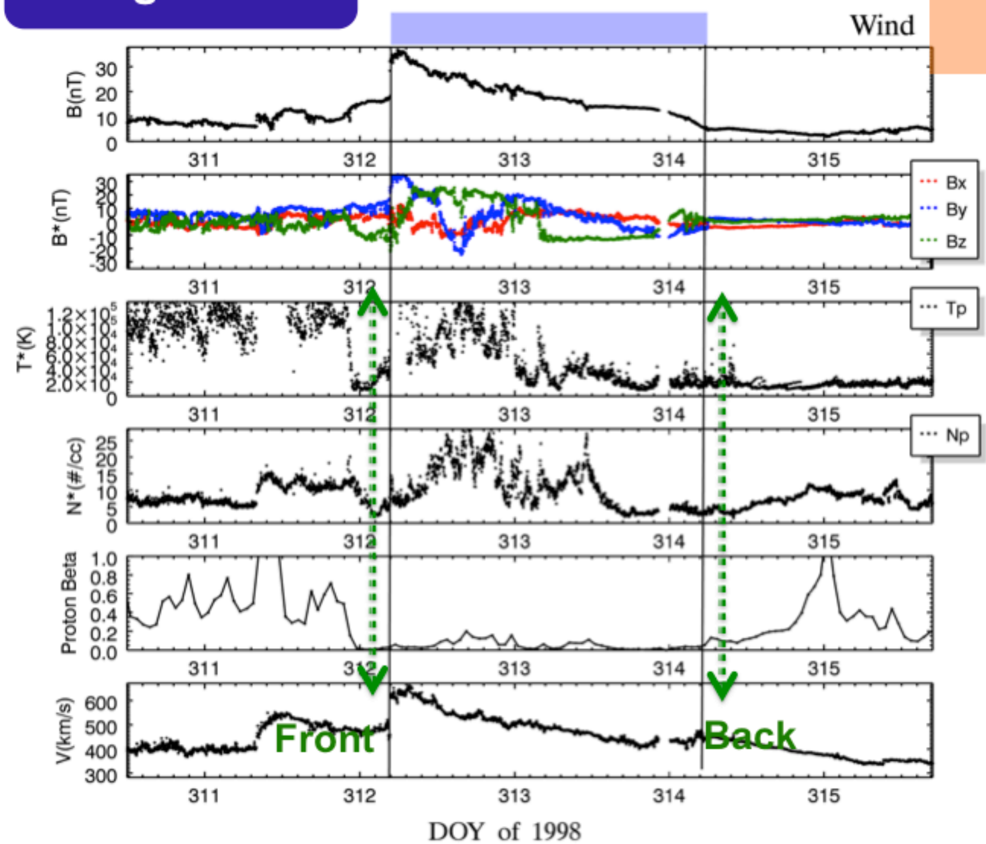

Wind ICME on May 18, 2002
Observed expansion velocity = 74 km/s

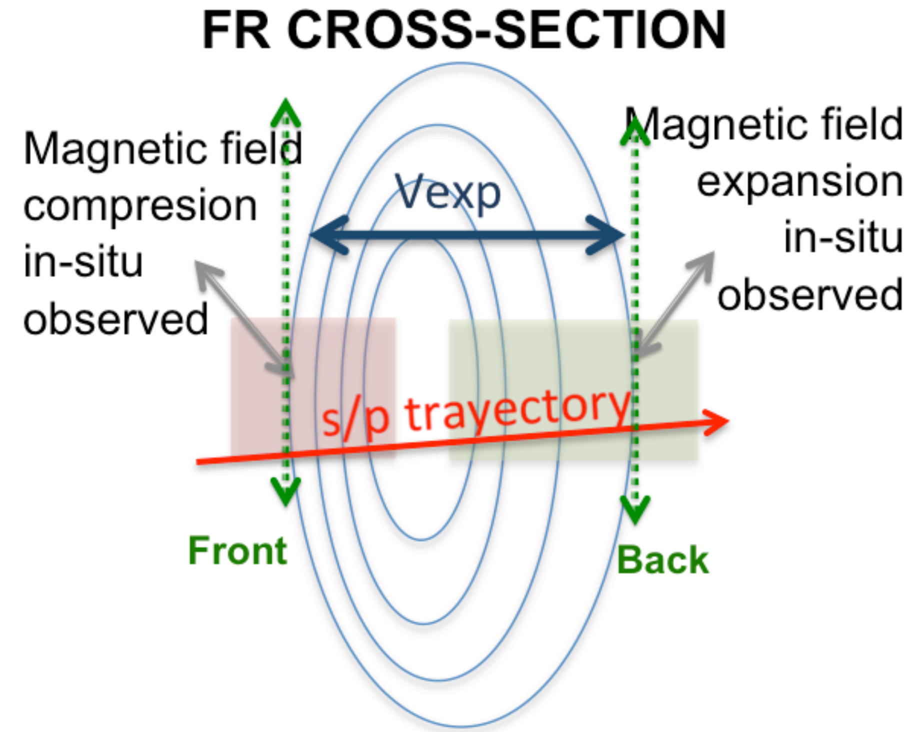

Q : Can we get information about the Magnetic Obstacle topology from the in-situ observations?

Earth-directed ICME magnetic field configurations

<u>Distortion Parameter (DIP)</u> is calculated from the integration in the time of the in-situ observed magnetic field magnitude inside of the Flux-Rope.

DIP is the value of the *Normalized Time* where *F* is equal to $F_{total}/2$.

- DIP = 0.5 is <u>symmetric</u> magnetic field magnitude.
- DIP > 0.5 is <u>back compression</u> magnetic field mag.
- DIP < 0.5 is <u>front compression</u> magnetic field mag.

$$F = \int_0^1 B\,dt$$

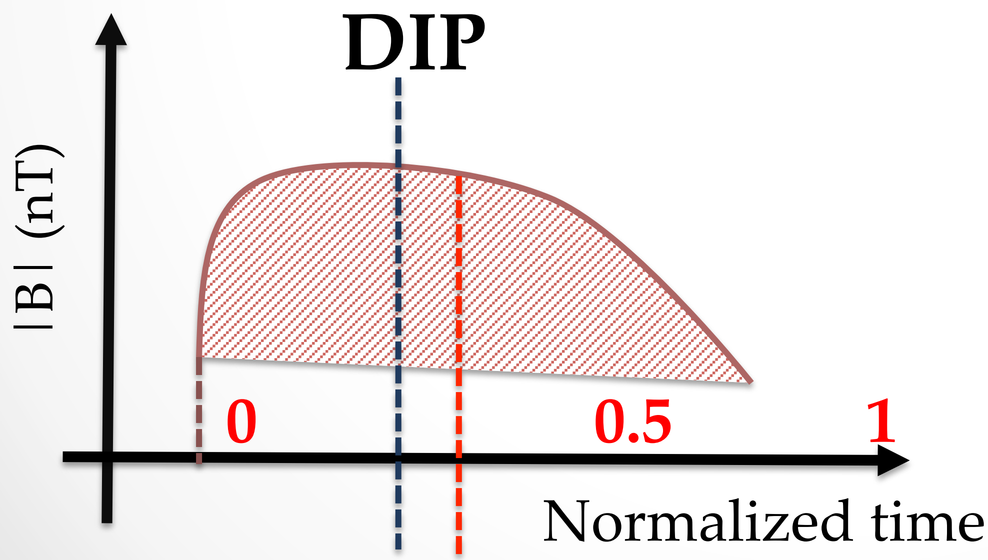

EXPANSION VEL.

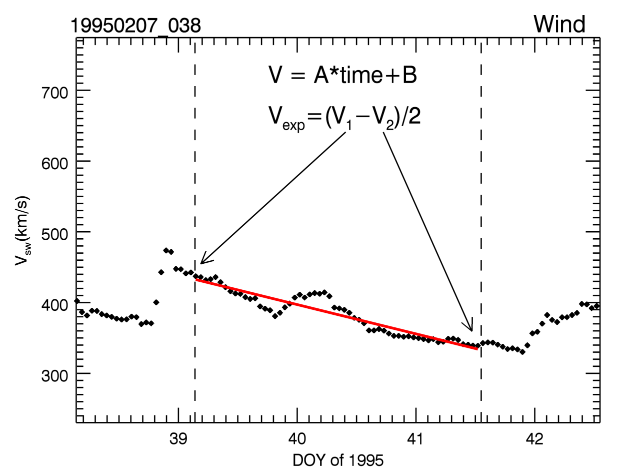

Gulisano et al.2010

Earth-directed ICME magnetic field configurations

http://wind.nasa.gov

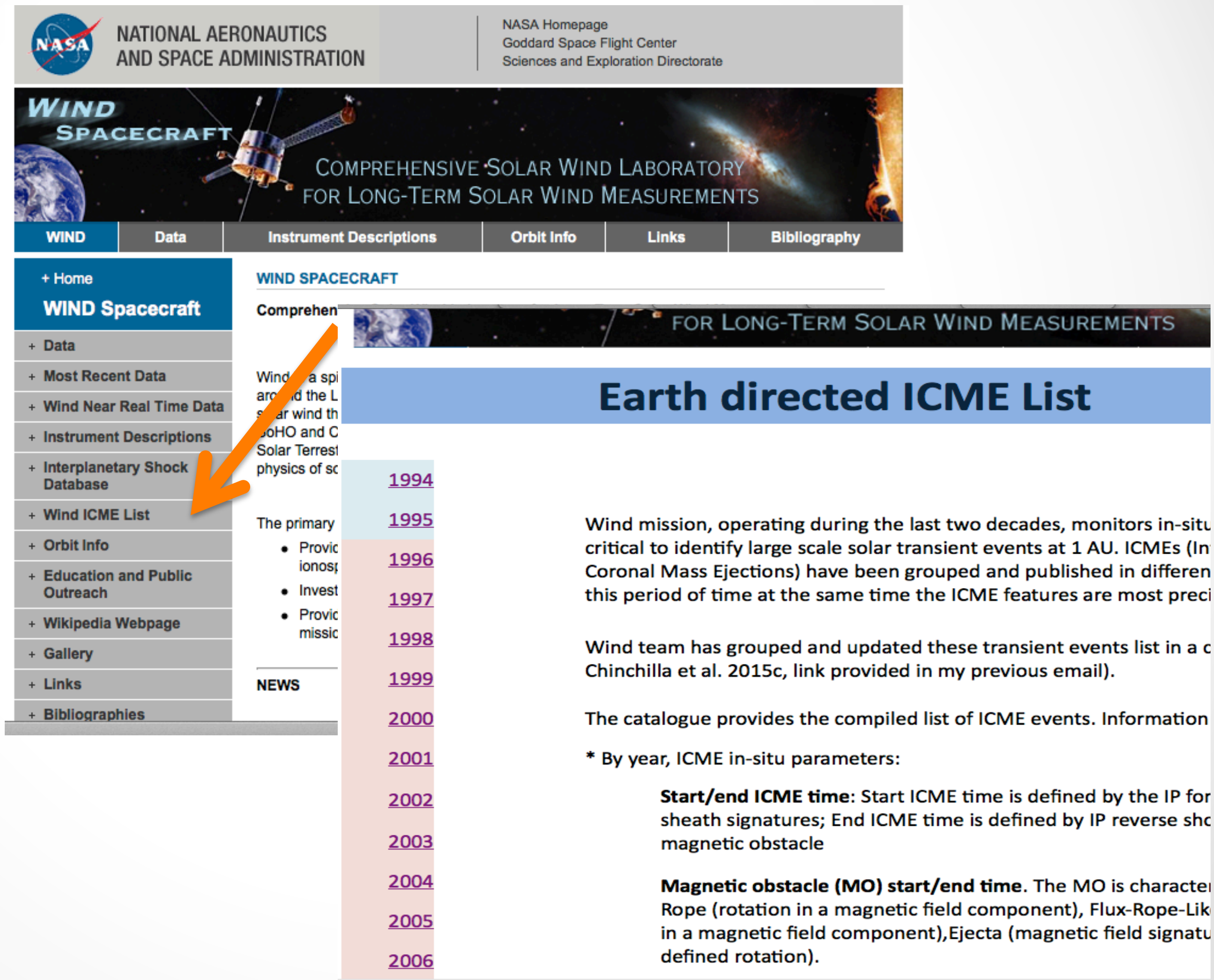

Wind ICME events 1995-2014

Cycle 23 (146)

Cycle 24 (241)

TOTAL (387)

Lepping et al. 1990
Nieves-Ch. et al. 2005
Lepping et al. 2008
Richardson & Cane, 2010
Lepping et al. 2010
Kilpua et al. 2012

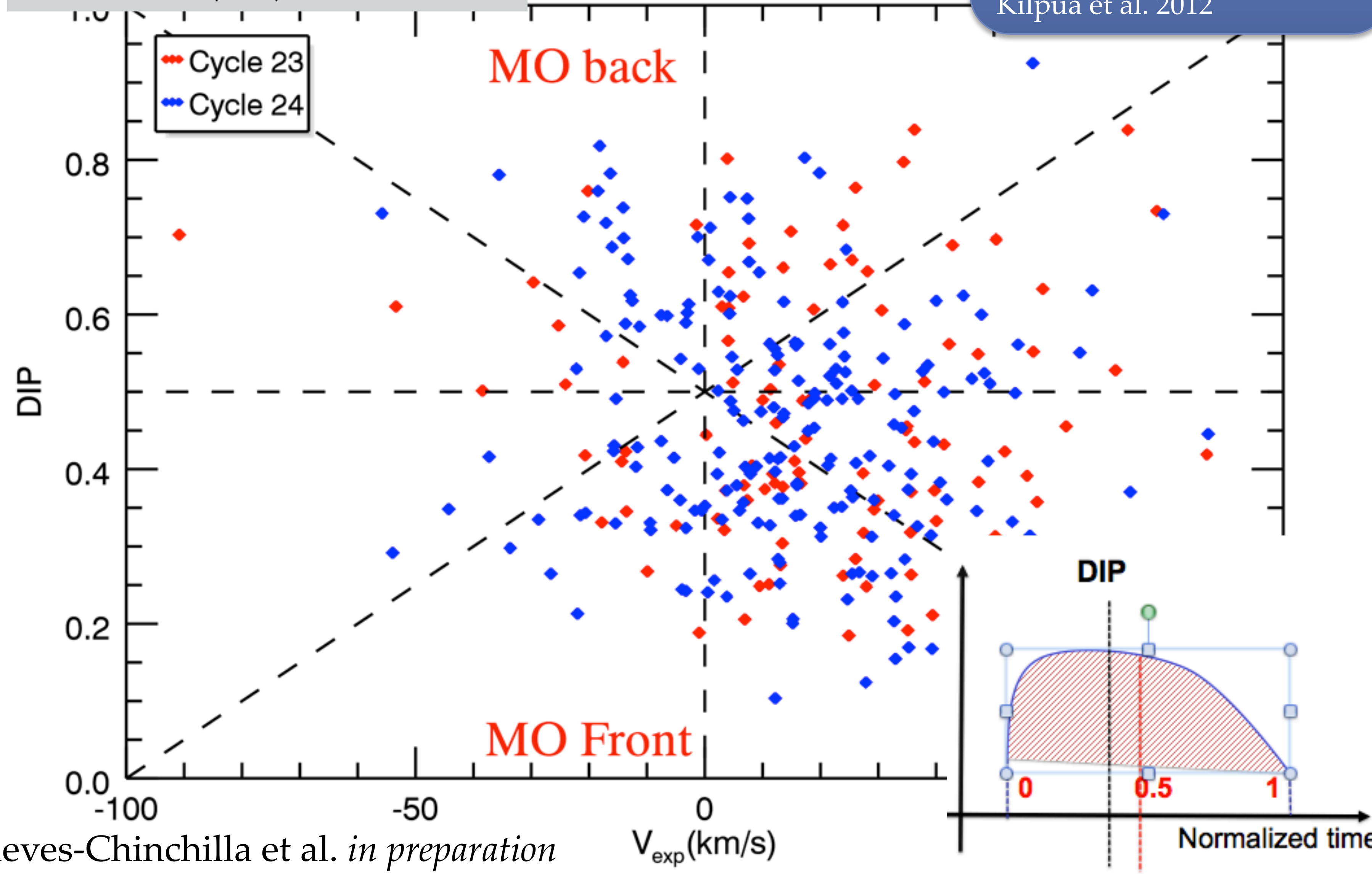

Nieves-Chinchilla et al. *in preparation*

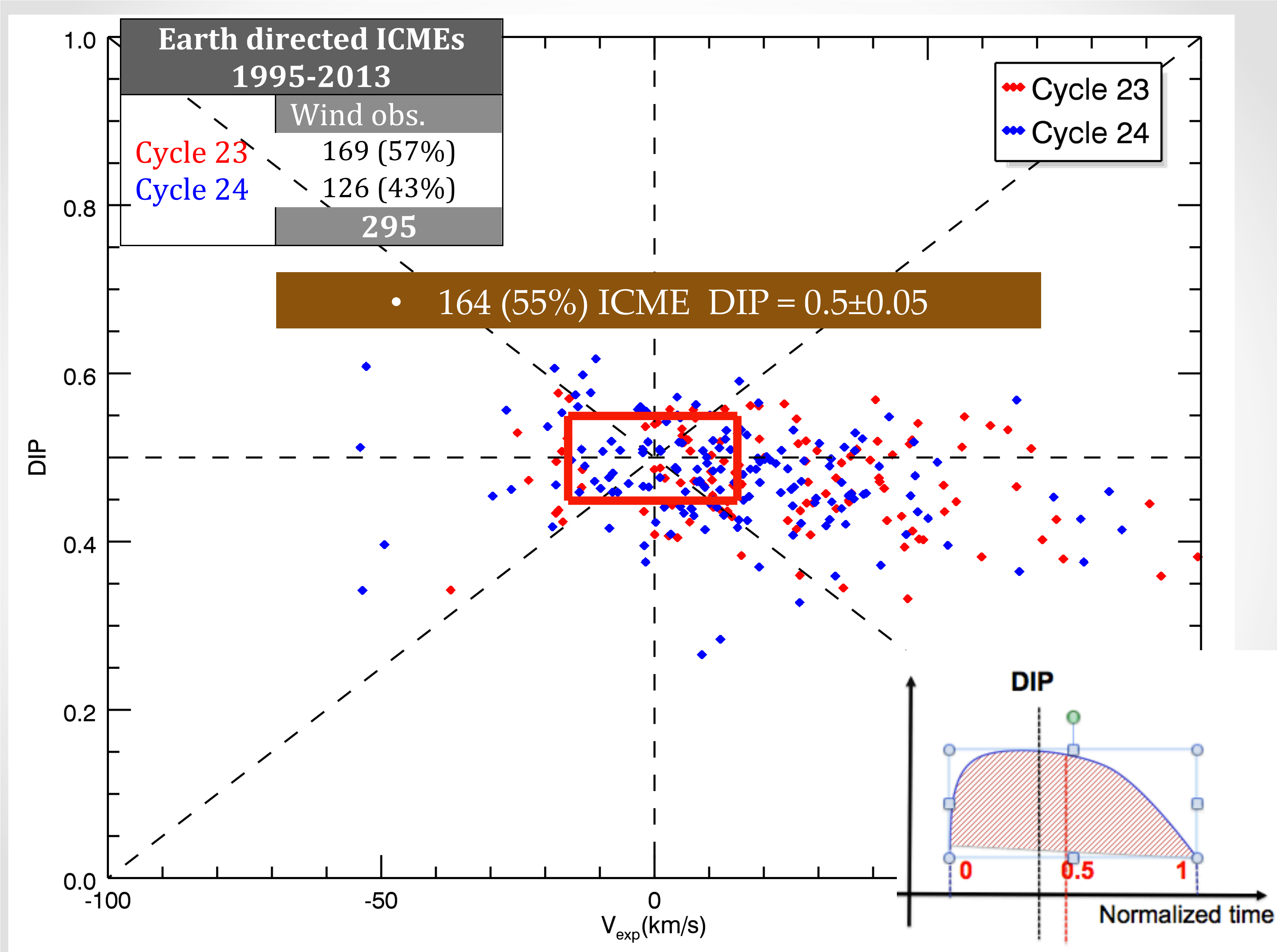

Earth directed ICMEs
1995-2013
Wind obs.
Cycle 23 169 (57%)
Cycle 24 126 (43%)
295
Cycle 23
Cycle 24
• 164 (55%) ICME DIP = 0.5±0.05
DIP
1.0
0.8
0.6
0.4
0.2
0.0
-100
-50
0
V_{exp}(km/s)
DIP
0
0.5
1
Normalized time

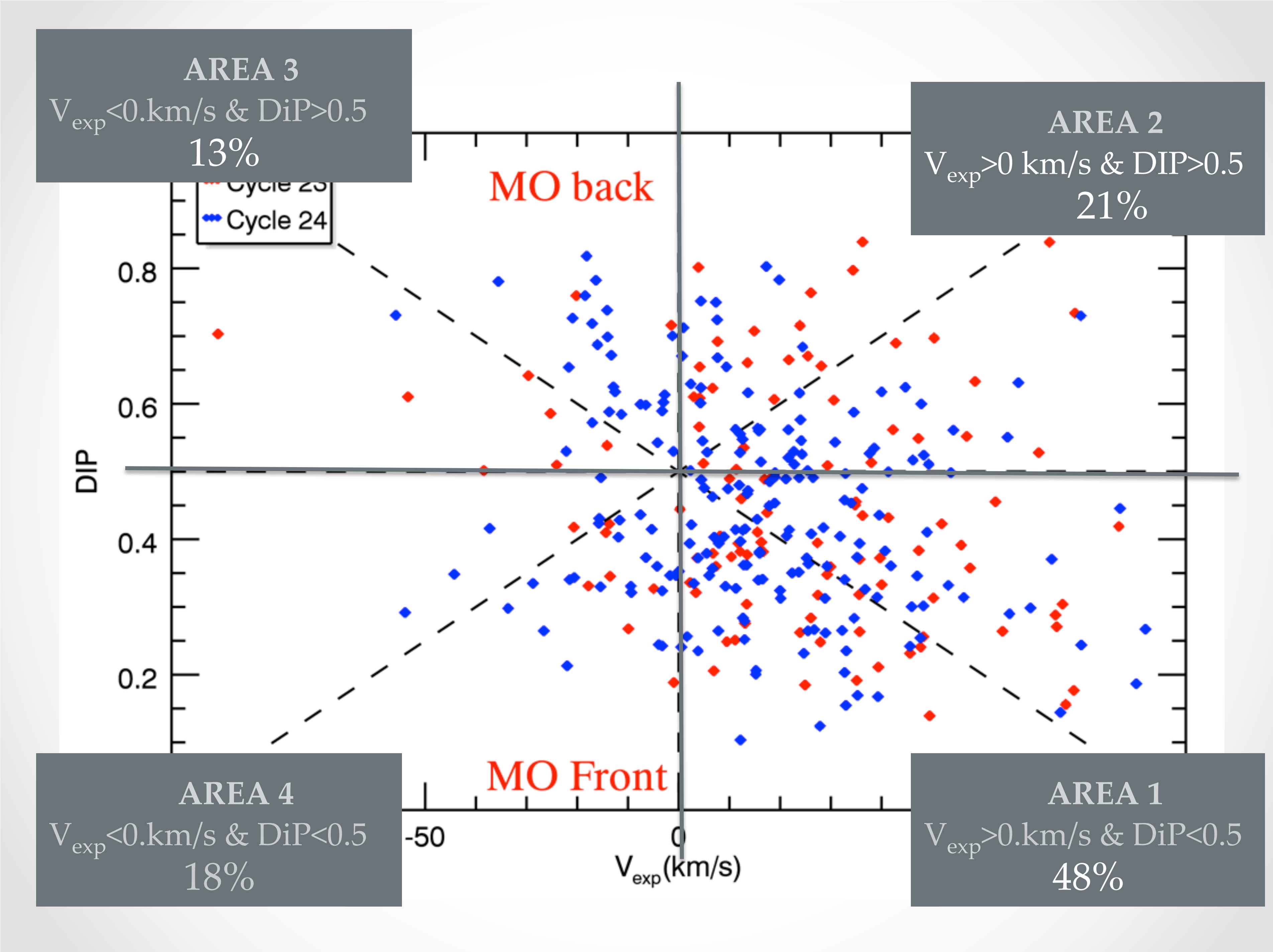

AREA 3
V_exp<0.km/s & DiP>0.5
13%
AREA 2
V_exp>0 km/s & DIP>0.5
21%
MO back
Cycle 24
0.8
0.6
DIP
0.4
0.2
AREA 4
V_exp<0.km/s & DiP<0.5
18%
MO Front
-50
0
V_exp(km/s)
AREA 1
V_exp>0.km/s & DiP<0.5
48%

C23 => 67 events (37% of A1 Total) $\langle V_{exp} \rangle$ = 39 km/s
C24 => 113 events (63% of A1 Total) $\langle V_{exp} \rangle$ = 34 km/s

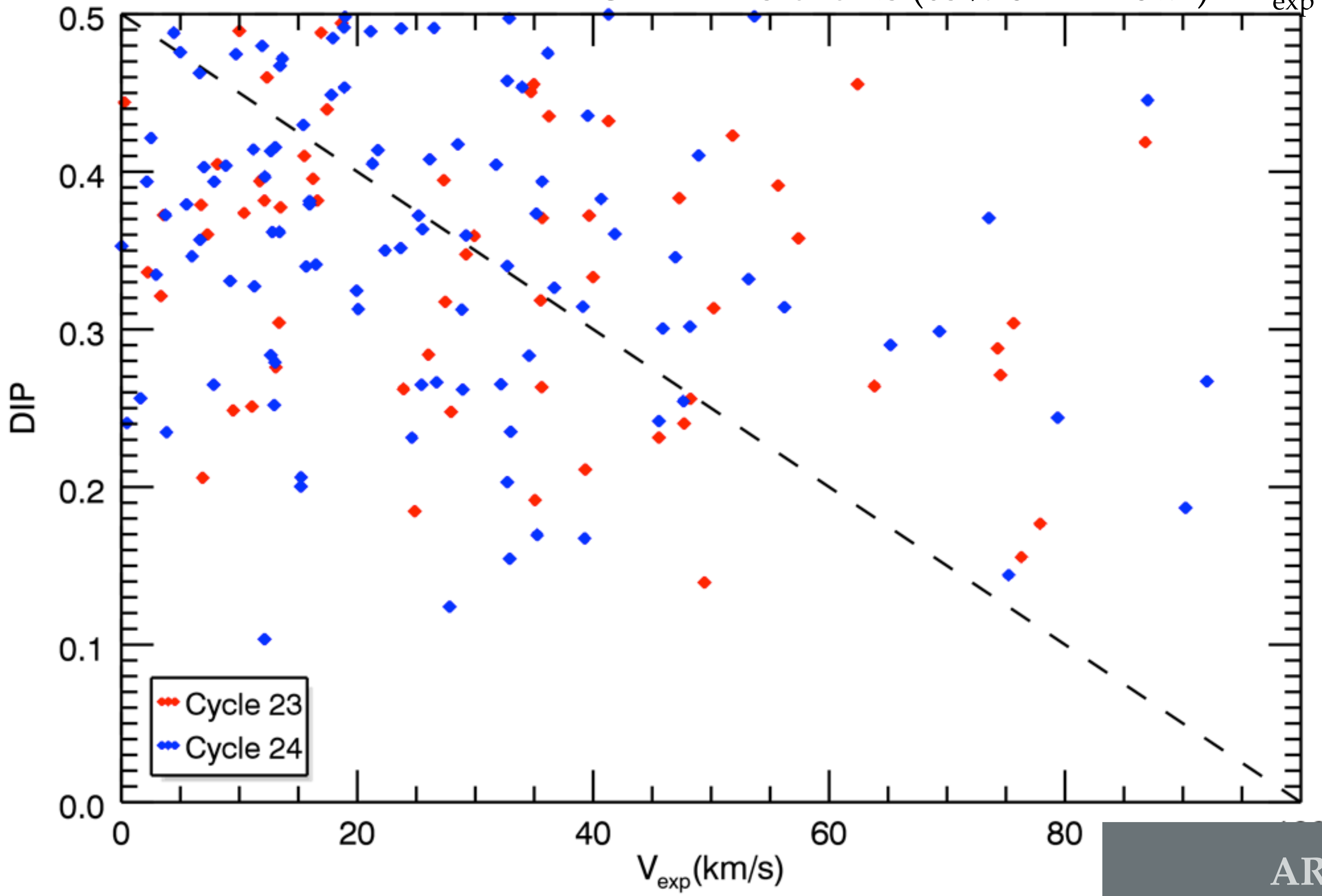

AREA 1

V_{exp}>0.km/s & DiP<0.5

48%

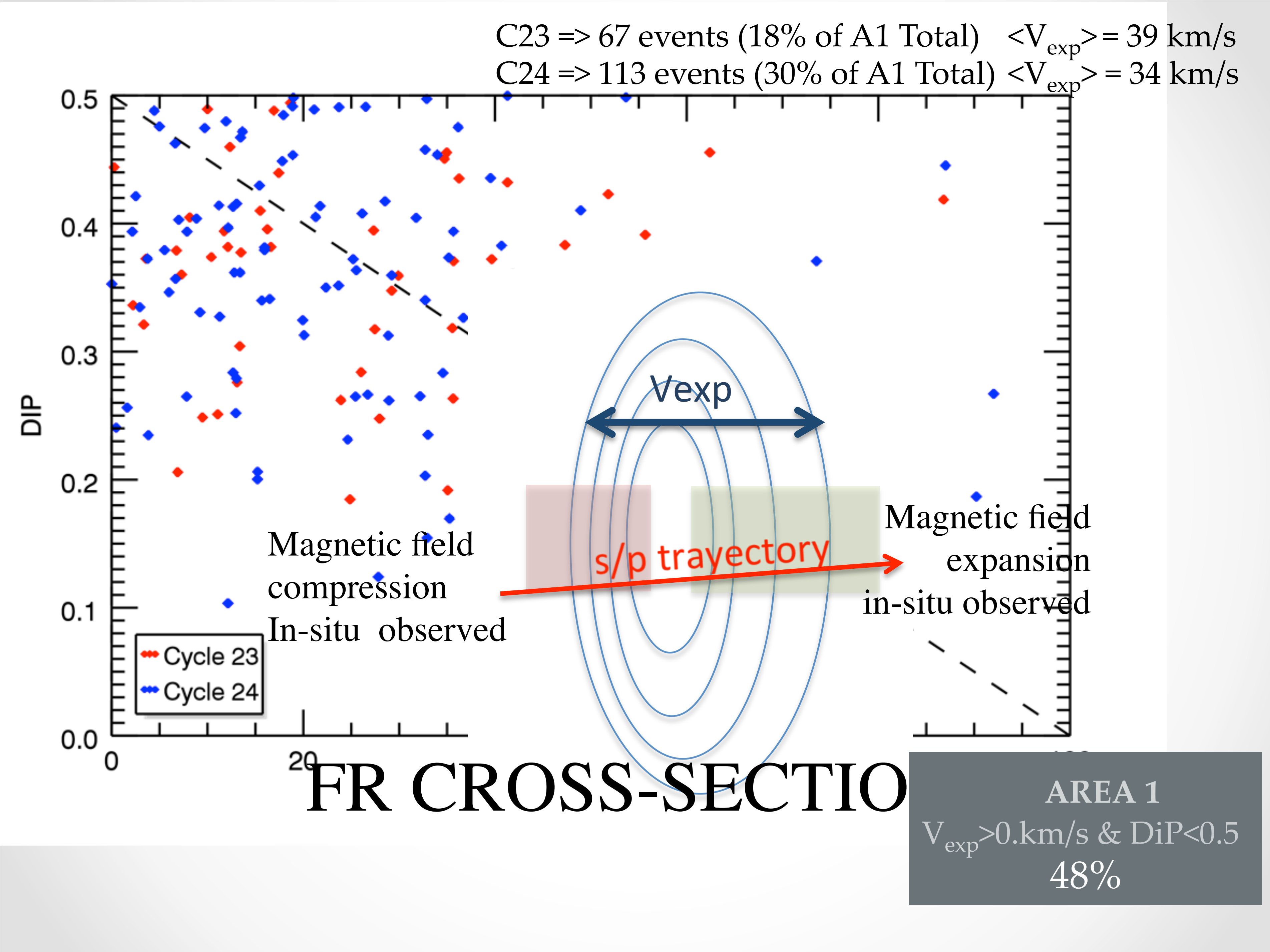

C23 => 67 events (18% of A1 Total) <Vexp>= 39 km/s
C24 => 113 events (30% of A1 Total) <Vexp> = 34 km/s
DIP
0.5
0.4
0.3
0.2
0.1
0.0
0
20
Cycle 23
Cycle 24
Vexp
s/p trayectory
Magnetic field compression In-situ observed
Magnetic field expansion in-situ observed
FR CROSS-SECTIO
AREA 1
Vexp>0.km/s & DiP<0.5
48%

C23 => 32 events (8% of C23 Total) $\langle V_{exp} \rangle$ = 25 km/s
C24 => 24 events (13% of C24 Total) $\langle V_{exp} \rangle$ = 19 km/s

AREA 2
V_{exp}>0 km/s & DIP>0.5
21%

Figure 3

Wind ICME on Nov 17, 2008
Observed V_{exp} = 53 km/s

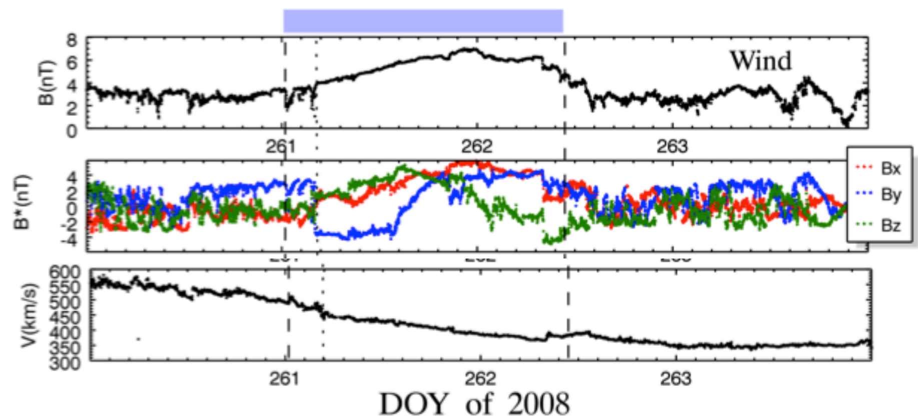

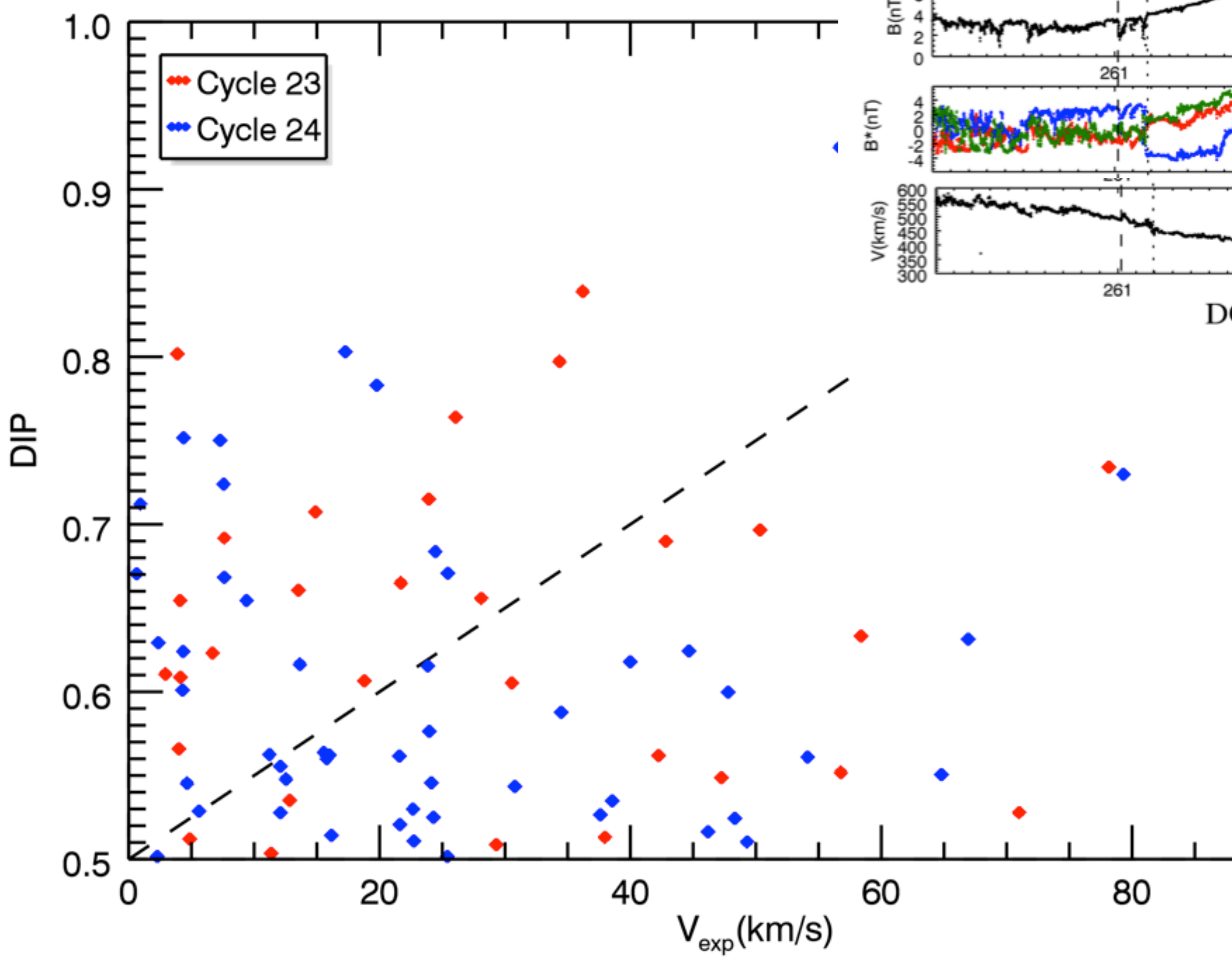

C23 => 32 events (8% of C23 Total) <V_{exp}> = 25 km/s
C24 => 24 events (13% of C24 Total) <V_{exp}> = 19 km/s

AREA 2
V_{exp}>0 km/s & DIP>0.5
21%

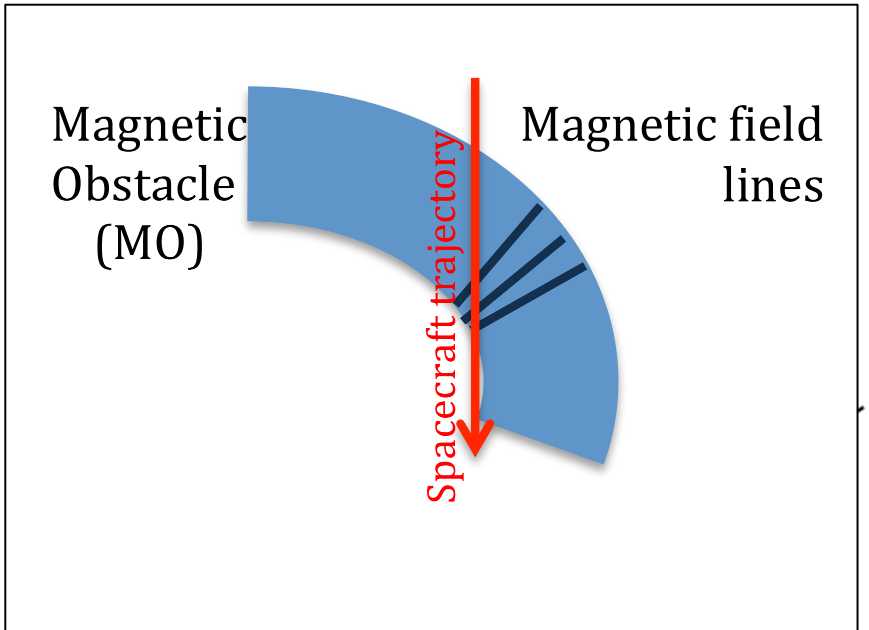

Figure 3

Wind ICME on Nov 17, 2008
Observed V_{exp} = 53 km/s

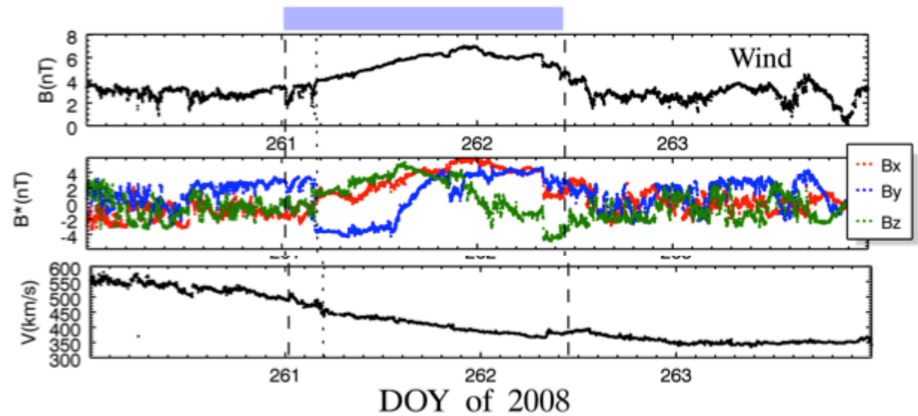

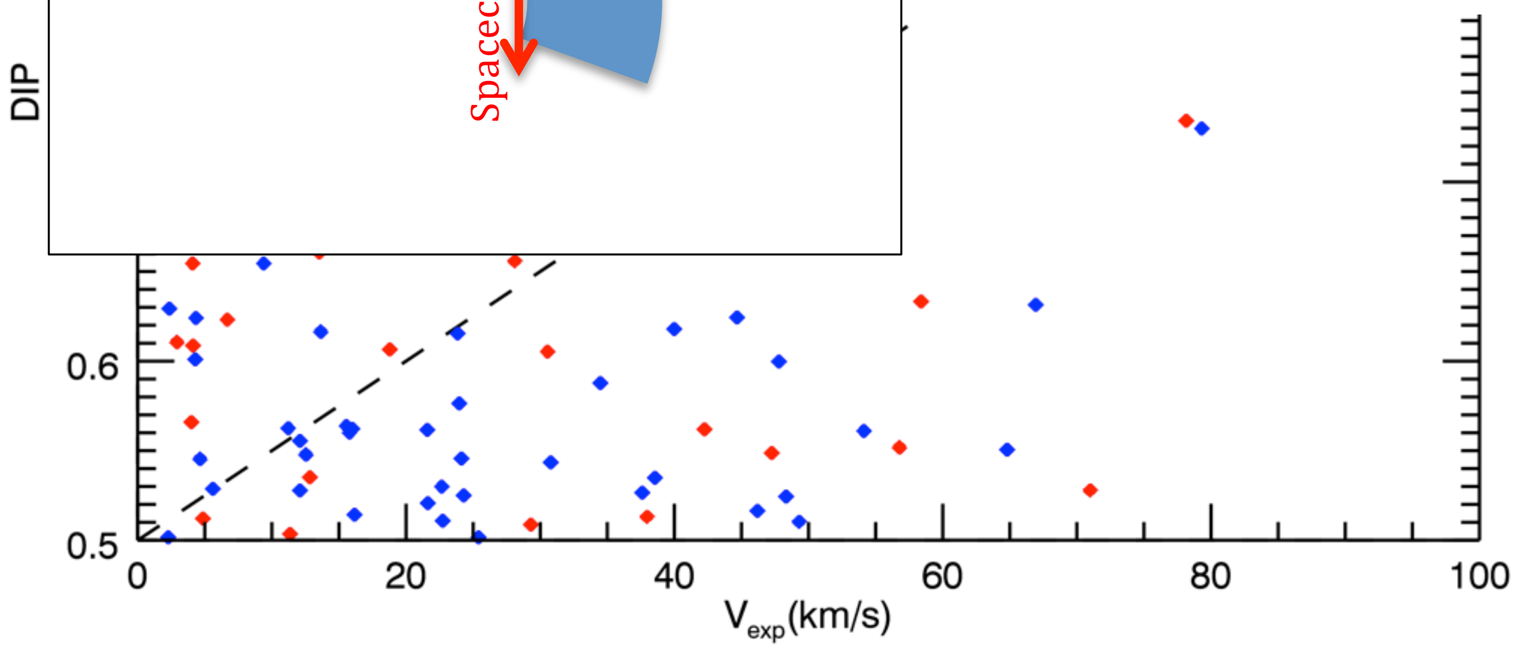

AREA 3

V_{exp}<0.km/s & DiP>0.5

13%

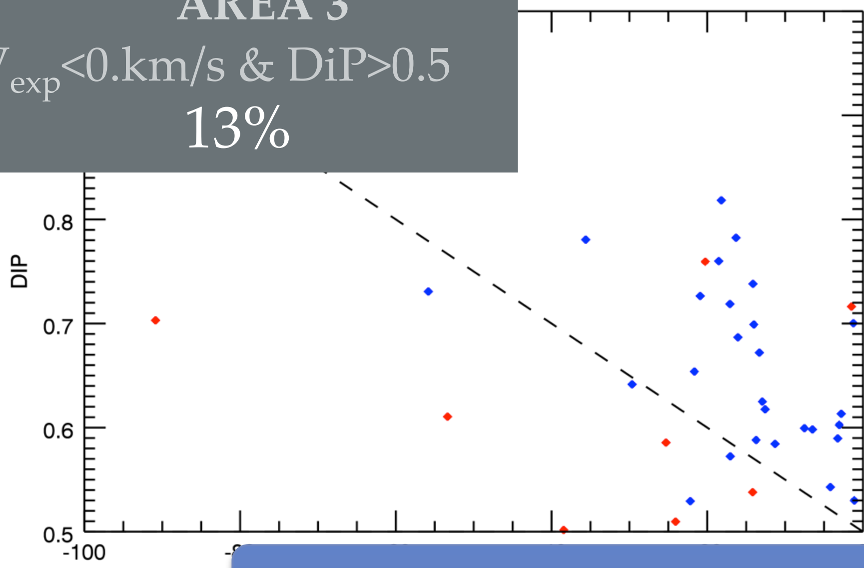

Wind - 20110429 119

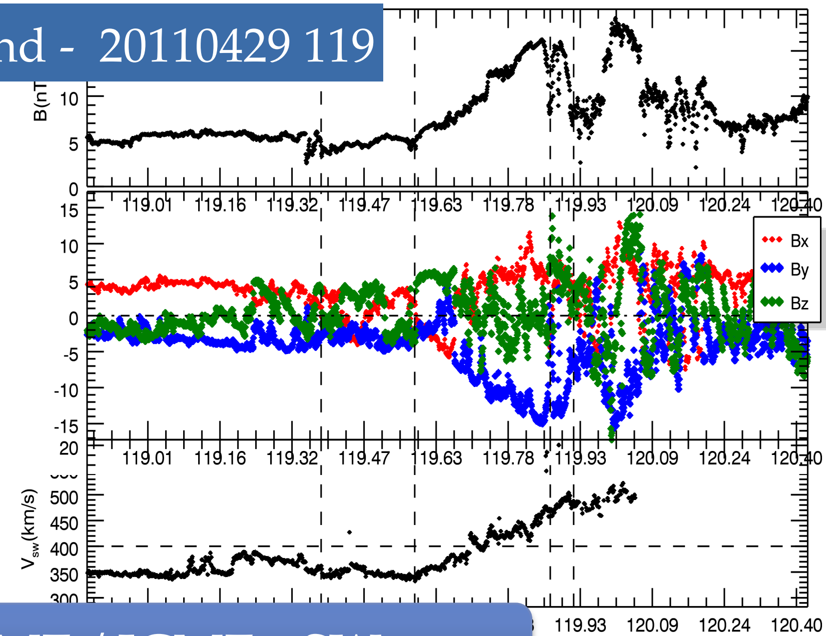

INTERACTION CME – CME / ICME - SW

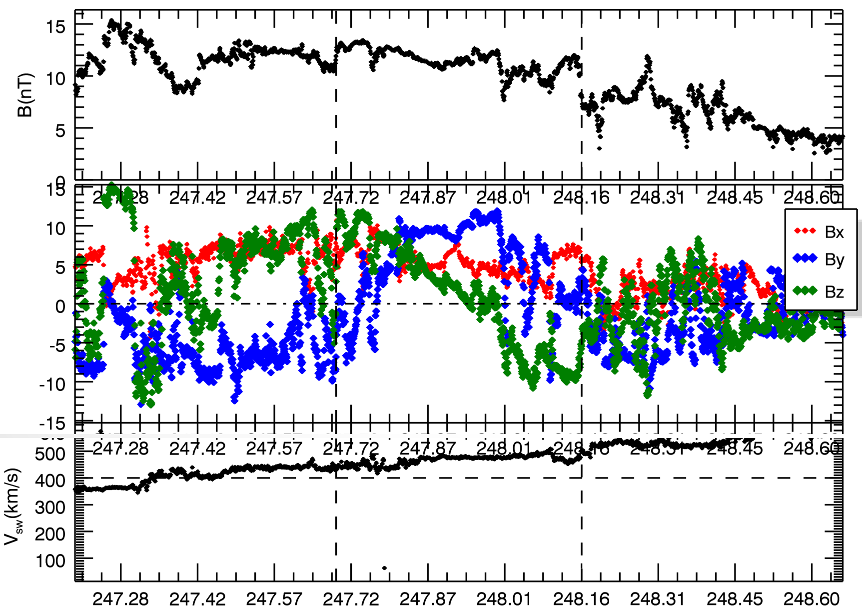

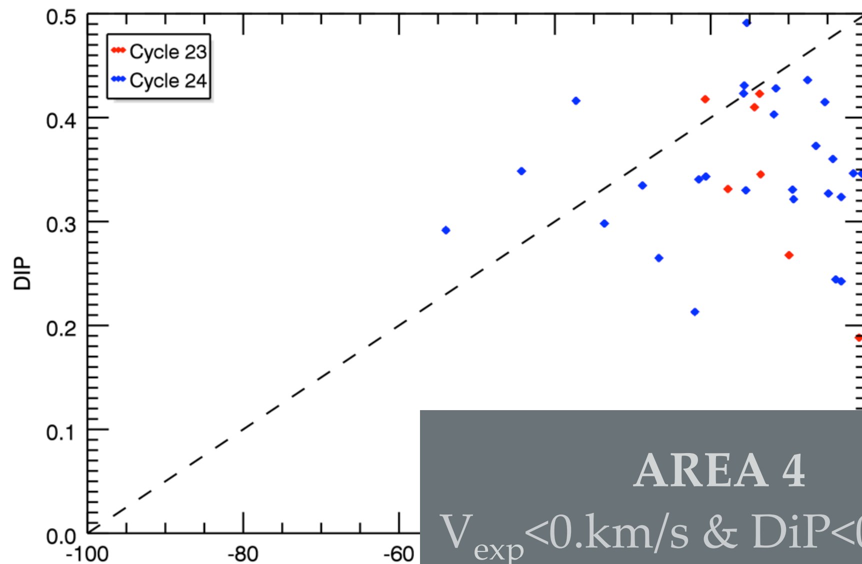

AREA 4

V_{exp}<0.km/s & DiP<0.5

18%

Can we get information about the Magnetic Obstacle topology from the in-situ observations?

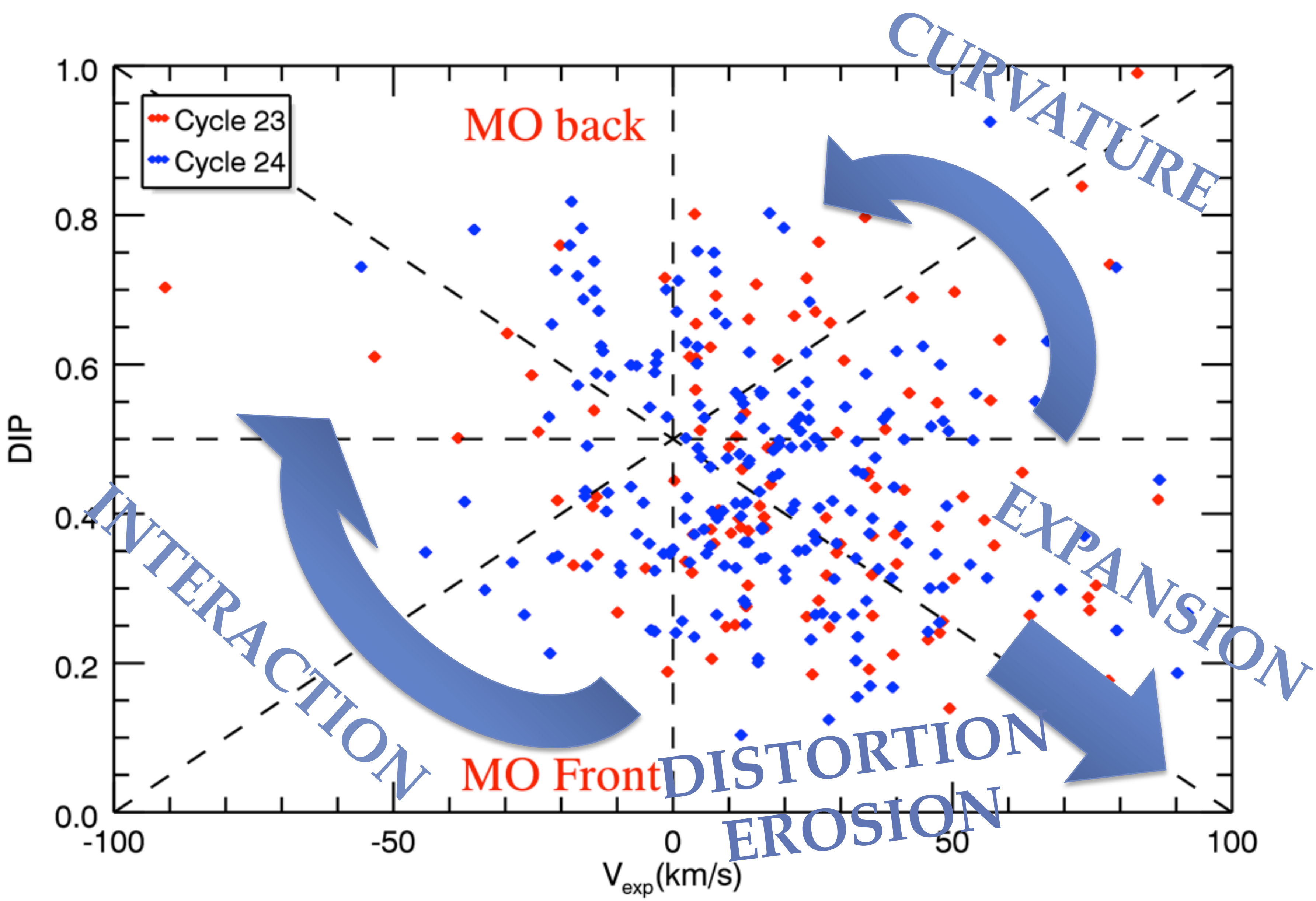

Some events from WG4

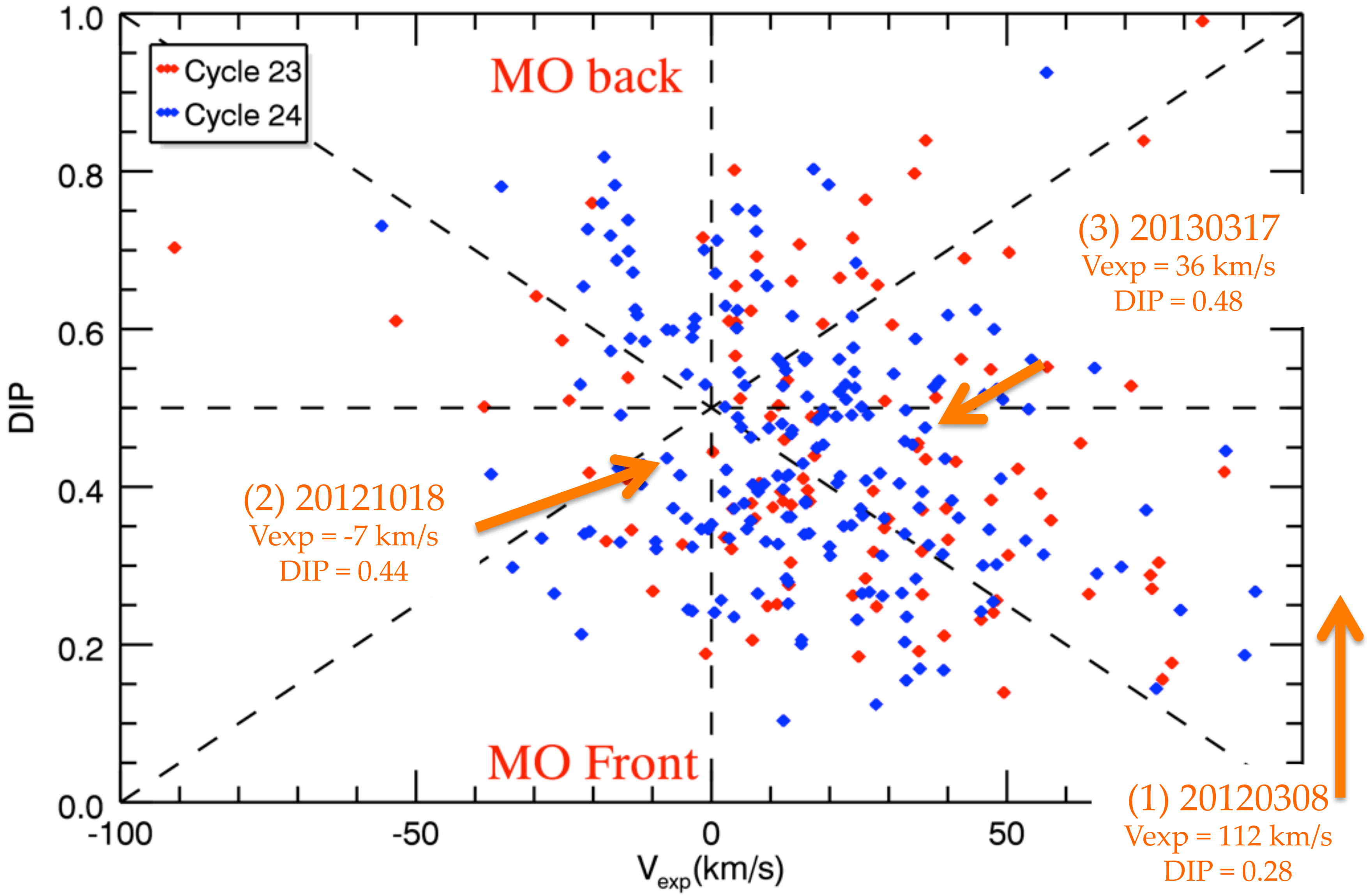

Summary & Conclusions

- A **real flux-rope** could be defined as magnetized plasma contained within a closed structure with magnetic field lines wrapping around in a twisting and disordered way.
- Despite multipoint and multi-view observations, the **reconciliation** between the in-situ and imaging interpretations of these 3D structures remains open.
- Empirical models for flux-ropes in the low corona are linked with in-situ analytical models through forward modeling techniques that provide geometrical and kinematic parameters.
- It is a challenge to conciliate the magnetic field topology view from 3D MHD simulations with the the neat, and helically well-organized magnetic field lines reconstructed with current in-situ analytical models.
- To learn about the Magnetic Obstacle topology from the in-situ observations, we have developed a parameter (Distortion Parameter, DIP).
- DIP vs expansion velocity analysis evidences that more effects than expansion should be included (*Models On Demand*) as curvature, interaction …